1   **Group A *Streptococcus* coordinates manganese import and iron efflux in response to**

2   **hydrogen peroxide stress**

3

4   Andrew G. Turner[1], Karrera Y. Djoko[1,3], Cheryl-lynn Y. Ong[1,2], Timothy C. Barnett[4], Mark

5   J. Walker[1,2,*], Alastair G. McEwan[1,2,*]

6

7   [1]School of Chemistry and Molecular Biosciences and [2]Australian Infectious Diseases

8   Research Centre, The University of Queensland, St Lucia 4072, Australia; [3]Department of

9   Biosciences, Durham University, DH1 3LE, UK, [4]Telethon Kids Institute, The University of

10   Western Australia, Nedlands 6009, Australia.

11

12   To whom correspondence should be addressed: Prof. Alastair McEwan, School of Chemistry

13   and Molecular Biosciences, The University of Queensland, Cooper Road, St Lucia, QLD,

14   4072, Australia. mcewan@uq.edu.au, Tel: +61-7-3346 0503; Prof. Mark Walker, School of

15   Chemistry and Molecular Biosciences, The University of Queensland, Cooper Road, St

16   Lucia, QLD, 4072, Australia. mark.walker@uq.edu.au, Tel: +61-7-33461623

17

18   [*]**Contributed equally to this work**

19

22

Abstract

Bacterial pathogens encounter a variety of adverse physiological conditions during infection, including metal starvation, metal overload and oxidative stress. Here we demonstrate that group A *Streptococcus* (GAS) utilizes Mn(II) import *via* MtsABC during conditions of hydrogen peroxide stress to optimally metallate the superoxide dismutase, SodA, with Mn. MtsABC expression is controlled by the DtxR-family metalloregulator MtsR, which also regulates expression of Fe uptake systems in GAS. Our results indicate that the SodA in GAS requires Mn for full activity and has lower activity when it contains Fe. As a consequence, under conditions of hydrogen peroxide stress where Fe is elevated we observed that the PerR-regulated Fe(II) efflux system PmtA was required to reduce intracellular Fe, thus protecting SodA from becoming mismetallated. Our findings demonstrate the coordinate action of MtsR-regulated Mn(II) import by MtsABC and PerR-regulated Fe(II) efflux by PmtA to ensure appropriate Mn(II) metallation of SodA for optimal superoxide dismutase function.

Introduction

Trace transition metals are important bacterial nutrients but can be toxic in excess. The concentration of available metal ions is tightly regulated in the host (1), particularly for Fe and Zn, which are sequestered within host tissues as pathogen control strategies (2). In addition to metal starvation, bacteria are also subject to killing *via* metal overload within innate immune cells. Examples include Cu- and Zn- dependent killing of *Salmonella* (3, 4) and *Mycobacterium tuberculosis* within macrophages (5, 6), and Zn-dependent killing of *Streptococcus pyogenes* within neutrophils (7). Bacteria also experience oxidative and nitrosative stress arising from reactive oxygen and nitrogen species (ROS and RNS) generated by innate immune cells, and bacterial pathogens have evolved defense systems that protect against these challenges (8). Importantly, there is close interplay between metal ion homeostasis and oxidative stress response. Metals such as Cu and Fe can cause toxicity by potentiating oxidative stress (9), while Mn is generally considered to have a protective role against ROS (10, 11).

S. pyogenes (group A *Streptococcus*, GAS) is an obligate human pathogen that causes a wide spectrum of diseases, ranging from mild infections of the pharynx and skin through to severe, life-threatening diseases such as necrotizing fasciitis and streptococcal toxic shock syndrome (12). GAS strains express a variety of virulence factors to subvert phagocytosis (13), abrogate immune responses, enhance inflammation (14), promote local tissue invasion (15), acquire metal ions (16), and defend against oxidative stress (17, 18). GAS uses superoxide dismutase (SOD) to detoxify the superoxide anion and, although it lacks catalase, it does possess peroxidases for the removal of hydrogen peroxide (H_2O_2) (18, 19). GAS encodes a single superoxide dismutase, SodA, which is thought to use Mn as a cofactor (20, 21) although it should be noted that cambialistic SODs capable of using either Mn or Fe have been described

1   in some Gram-positive bacteria, including *Streptococcus pneumoniae* and *Staphylococcus*

2   *aureus* (22, 23).

3

4   Given the differing pro- and anti- oxidant effects of Fe and Mn, it follows that GAS must

5   tightly coordinate Fe and Mn homeostasis to meet the intracellular demand for these metal

6   ions and maintain biochemical functions, while at the same time avoid the potential for

7   oxidative stress. In many Gram-positive bacteria, including GAS, the peroxide response

8   regulator PerR regulates the cellular response to oxidative stress and also contributes to Fe

9   and Mn homeostasis (17, 24-26). The Fe-loaded form of PerR is highly sensitive to oxidation

10 by H_2O_2, which in turn enables de-repression of genes involved in the oxidative stress

11 response (27). In GAS, these genes include *pmtA*, which encodes a P_{1B-4}-type ATPase that

12 effluxes ferrous iron and likely reduces the potentiating effects of excess Fe on H_2O_2 and

13 superoxide stress (28, 29). In contrast, Mn-loaded PerR is H_2O_2-insensitive and thus it

14 continues to repress the PerR regulon (30).

15

16 Mn import in GAS is mediated by the ABC-type metal transport system MtsABC and this

17 system is essential for protection against the superoxide generator, paraquat (21). The DtxR

18 family regulator MtsR functions as a repressor that senses cellular Mn levels in GAS and

19 regulates expression of MtsABC (21, 31). GAS lacks a Fur homolog and instead uses its Mn

20 sensor, MtsR, to also control Fe homeostasis *via* the expression of the haem acquisition

21 accessory proteins Shr and Shp, the haem importer SiaABC, and the ferric ferrichrome

22 importer SiuABDG (32-36). Recent findings in *Streptococcus cristatus* (formerly <u>S.</u>

23 <u>oligofermentans</u>) have shown that MntR, an MtsR homologue, can also act as a H_2O_2 sensor

24 and activate Mn import in response to H_2O_2 stress (37).

25

1   In this work, we examine the relationship between Mn import (*via* MtsABC and regulated by

2   MtsR), Fe efflux (*via* PmtA and regulated by PerR), and defense against oxidative stress (*via*

3   SodA) in GAS. We show that uptake of Mn occurs upon exposure to H_2O_2 and subsequently

4   leads to activation of SodA. This influx of Mn requires a functional MtsABC but does not

5   rely upon upregulation of *mtsABC* by MtsR. We further demonstrate that SodA from GAS is

6   more active in the Mn-metallated form when compared to the Fe-metallated form and that

7   optimal SodA activity also depends on a functional PmtA. These coordinated systems ensure

8   optimal Mn metallation of GAS SodA for oxidative stress defense.

9

10   **Experimental procedures**

11   **Bacterial strains and growth conditions**

12   The invasive GAS strain M1T1 clinical isolate 5448 was used in this study (38). 5448 wild-

13   type (WT) and isogenic mutant strains were routinely cultured at 37 °C in Todd-Hewitt broth

14   (Difco) supplemented with 1% w/v yeast extract (Merck) (THY). For growth on solid

15   medium, strains were cultured on horse blood agar (5% w/v) or THY agar (1.5% w/v).

16   *Escherichia coli* strains were grown in lysogeny broth (LB) (39). *E. coli* Top10 was used for

17   maintenance of pJRS233, pLZ12, and pBAD derived plasmids (Table S1). For selection in

18   GAS, the antibiotics kanamycin (300 μg/mL), spectinomycin (100 μg/mL), and erythromycin

19   (2 μg/mL) were used. Kanamycin (50 μg/mL), spectinomycin (100 μg/mL), and

20   erythromycin (500 μg/mL) were used to select for plasmids in *E. coli*.

21

22   **DNA manipulations and mutant construction**

23   All GAS mutant strains except 5448Δ*sodA* (see below) (Table S1) were constructed as

24   previously described (40). To construct the 5448Δ*mtsR* mutant, the 5' and 3' flanking regions

25   of *mtsR* was amplified using 5448 WT genomic DNA as templates and primer pairs mtsR-

KO-1 (incorporating an *Xho*I site at the 5' end) and mtsR-KO-2 (with homology to *aad9* (spec^R) at the 5' end), and mtsR-KO-3 (with homology to *aad9* at the 5' end) and mtsR-KO-4 (incorporating a *Bam*HI site at the 5' end), respectively (Table S2). The *aad9* cassette was amplified from pUCSpec using primers spec-F and spec-R. The resulting fragments were fused by 3-way PCR to form the mtsR-KO construct, which was ligated with the temperature-sensitive shuttle vector pJRS233. The pJRS233-mtsR-KO plasmid was electroporated into electrocompetent GAS as previously described (41). A double crossover event was selected for by serial passaging at 37 °C and 30 °C, resulting in 5448Δ*mtsR* that contains spec^R (marker) and has lost ery^R (shuttle vector). To generate the 5448Δ*mtsR::mtsR* complemented strain, the WT *mtsR* allele was amplified using primers mtsR-KO-1 and mtsR-KO-4, and ligated into pJRS233, yielding pJRS233-*mtsR*, which was electroporated into 5448Δ*mtsR*. The plasmid was integrated *via* double crossover at 37 °C for replacement of *aad9* with *mtsR* at the original locus, to yield 5448Δ*mtsR∶∶mtsR*.

Construction of 5448Δ*mtsABC* was achieved by amplification of the 5' and 3' flanking regions of *mtsABC* using 5448 WT template DNA and primer pairs mtsABC-KO-1 (incorporating an *Xho*I site at the 5' end) and mtsABC-KO-2 (with homology to *aphA-3* (km^R) at the 5' end), and primer set mtsABC-KO-3 (with homology to *aphA-3* at the 5' end) and mtsABC-KO-4 (incorporating a *Pst*I site at the 5' end), respectively (Table S2). The *aphA-3* gene was amplified from pUC4Ωkm2 using primers km-F and km-R. The resulting fragments were fused by 3-way PCR to form the mtsABC-KO construct, which was ligated into the temperature-sensitive shuttle vector pJRS233. The pJRS233-mtsABC-KO plasmid was electroporated into electrocompetent GAS and a double crossover event was selected for by serial passaging as described above, resulting in 5448Δ*mtsABC*. To generate the 5448Δ*mtsABC::mtsABC* complemented mutant, the WT *mtsABC* allele was amplified using

1 primers mtsABC-KO-1 and mtsABC-KO-4, and ligated into vector pJRS233, yielding

2 pJRS233-mtsABC, which was electroporated into 5448Δ*mtsABC*. The plasmid was

3 integrated *via* double crossover at 37 °C for replacement of km^R with *mtsABC* at the original

4 locus to yield 5448Δ*mtsABC∷mtsABC*.

5

6 Construction of 5448Δ*sodA* was achieved using the temperature-sensitive *E. coli*-GAS shuttle

7 vector pLZ12ts (Barnett *et al*., manuscript in preparation). The genomic regions flanking

8 *sodA* from 5448 WT amplified using primer pairs sodA-1 and sodA-2 (5'), and sodA-3 and

9 sodA-4 (3'). The kanamycin resistance cassette was amplified from pUC4ΩKm2 using

10 primers km-sodA-F and km-sodA-R which also shared homology to the *sodA* gene (Table

11 S2). pLZ12ts was amplified using primers pLZ12-F and pLZ12-R. The four PCR products

12 and linearised vector were assembled using the NEBuilder system (New England Biolabs)

13 according to manufacturer's directions, and the resultant plasmid was sub-cloned *E. coli*

14 Top10. The plasmid was electroporated into electrocompetent GAS and double crossover

15 mutants were selected for as described above, resulting in 5448Δ*sodA* that contains the km^R

16 (marker) and has lost spec^R (shuttle vector).

17

18 Construction of a plasmid for expression of GAS SodA was achieved through site-directed

19 mutagenesis of pBAD-myc-His-A to remove the myc epitope and insert a TEV protease cut

20 site upstream of the C-terminal 6xHis tag, using primer pairs pBAD-site-F and pBAD-site-R.

21 The resulting plasmid, pBAD-TEV-His, was digested with *Nco*I and *Apa*I, and ligated to a

22 *sodA* PCR fragment, which was prepared as follows. The *sodA* gene was amplified from

23 5448 WT using primers sodA-prot-F (incorporating a *Nco*I cut site at the 5' end) and sodA-

24 prot-R (incorporating an *Apa*I cut site at the 5' end). Then resultant PCR product was then

25 digested with *Nco*I and *Apa*I and ligated into pBAD-TEV-His, and transformed into *E. coli*

1 Top10. All strains were confirmed by DNA sequencing (Australian Equine Genetics

2 Research Centre, The University of Queensland).

3

4 **Analyses of intracellular metal content**

5 For analysis of intracellular Mn accumulation, GAS strains were grown in THY to OD_{600} 0.6-

6 0.8 and challenged for 1 h with either 8 mM Fe(II) or 1 mM Mn(II). Sterile deionised water

7 was used as a control. For metal accumulation following H_2O_2 exposure, strains were grown

8 in THY to OD_{600} 0.6-0.8. Following collection of the T_0 aliquot, the strains were challenged

9 for 30 min with either sterile water, 1 mM, or 4 mM H_2O_2. Alternatively, for experiments

10 examining metal accumulation profiles due to regulator deletion, strains were grown to OD_{600}

11 0.6-0.8 in THY alone. For experiments to establish metal accumulation profile, strains were

12 grown in THY alone or in the presence of 2,2'-bipyridyl (20 µM), Fe(II) (20 µM, 200 µM, or

13 2 mM), and/or Mn(II) (20 µM).

14

15 Cells were spun at 3,200 x g at 4°C for 15 min and washed three times in 1X PBS containing

16 250 mM EDTA, followed by 3 washes in 1X PBS, and a sample was taken to determine total

17 protein content by BCA assay (Thermo Scientific). Samples were digested in 70% nitric acid

18 at 70 °C for 48 h, diluted to 2% nitric acid with HPLC grade H_2O, and analysed for Fe and

19 Mn by inductively-coupled plasma mass-spectrometry (ICP-MS) at the School of Earth and

20 Environmental Sciences at the University of Queensland. Metal content was normalised to

21 total protein content obtained from the BCA assay.

22

23 Metal content of rSodA proteins was assessed by ICP-MS. Briefly, protein concentrations of

24 rSodA-Fe and rSodA-Mn isoforms were obtained by BCA assay and solutions of each

25 protein were adjusted to a final concentration of 10, 20, or 40 nM in HPLC-grade H_2O with

1   2% HNO_3. Total parts per billion values for metal were converted to nM in sample to

2   establish molar equivalents of bound metal.

3

4   **Viability of cells during hydrogen peroxide challenge**

5   GAS strains were grown in THY to $OD_{600} = 0.6$-0.8. Upon collection of a T_0 sample, cultures

6   were challenged with water, 1 mM H_2O_2, or 4 mM H_2O_2, and incubated at 37 °C for 30 min.

7   Following incubation, cultures were vortexed for 30 s, serially diluted, and plated onto THY

8   agar plates to assess viable colony-forming units (CFUs).

9

10   **Growth analysis**

11   Bacterial growth was assessed in the presence of varying amounts of Fe(II) ($FeSO_4 \cdot 7H_2O$),

12   Mn(II) ($MnSO_4 \cdot 4H_2O$), Zn(II) ($ZnSO_4 \cdot 7H_2O$), streptonigrin (Sigma), and methyl viologen

13   (paraquat; Sigma). All salts were analytical grade (Sigma). Metal solutions were prepared in

14   deionised distilled water and filter-sterilised. Streptonigrin was prepared in 100% ethanol and

15   paraquat in distilled deionised water. Overnight cultures of GAS grown in THY were diluted

16   in fresh THY to $OD_{600} = 0.05$ and supplemented with varying concentrations of each

17   compound. Cultures were grown in flat-bottom 96-well plates (Greiner; final volume of 200

18   μL/well) without shaking at 37 °C and optical densities at 595 nm were measured every 30

19   min using a FLUOstar Optima plate reader (BMG Labtech). Doubling time was calculated

20   using the reciprocal of the gradient of natural log-transformed OD_{595} values during

21   exponential growth phase.

22

23   **RNA extraction and qPCR analysis**

24   Overnight GAS cultures were diluted to $OD_{600} = 0.025$ in THY broth with or without 2 mM

25   Fe(II) or 0.5 mM Mn(II). At $OD_{600} = 0.6$-0.8, 5 mL of culture was harvested by

centrifugation (8,000 x g, 10 min). Bacterial pellets were immediately resuspended in TRIzol

(Invitrogen), transferred to lysing matrix B tubes (MP Biomedicals), and mechanically lysed

using the FastPrep 120 instrument (Thermo Scientific). Chloroform (0.2 volumes) was added

and the mixture was centrifuged (12,000 x g, 30 min, 4 °C). The aqueous phase was

removed, supplemented with 70% ethanol, and loaded onto RNeasy columns (QIAGEN) for

purification following manufacturer's recommendations. RNA was eluted in ultrapure water

and contaminating genomic DNA was removed using RNase-free DNase (TURBO,

Ambion). RNA integrity was examined by gel electrophoresis, and quantified by

spectrophotometric analysis on the NanoDrop instrument (Thermo Scientific).

RNA (500 ng) was converted to cDNA using random hexamers and Superscript VILO

(Invitrogen) following manufacturer's directions. qPCR was performed using SYBR Green

mastermix (Applied Biosystems) with 100 nM primer mixes (Table S2) and 2 ng cDNA per

reaction using an Applied Biosystems Quantistudio 6 instrument. Data were analysed using

LinRegPCR (42) to obtain Cq values with *gyrA* as the reference gene, and data plotted as

$\Delta\Delta$Cq (Log$_2$FC) (43) using 5448 WT in THY alone as the control, or WT at OD$_{600}$ = 0.3

(early exponential phase), OD$_{600}$ = 0.6 (mid-exponential phase), or OD$_{600}$ = 0.9 (late

exponential) for experimentation with 5448$\Delta perR$.

Expression of rSodA

E. coli Top10 containing pBAD-Sod-TEV-His was cultured in 500 mL LB containing 100

µg/mL ampicillin supplemented with either 250 µM Fe(II) or Mn(II) at 37 °C with vigorous

agitation. At OD$_{600}$ = 0.5, *L*-arabinose was added to a final concentration of 0.2% and cultures

were shifted to 28 °C for a further 4 h. Cells were harvested by centrifugation (5,000 x g,

4°C, 15 min), resuspended in buffer A (50 mM Tris pH 8.5, 150 mM NaCl, 5% glycerol)

1 containing protease inhibitors (Roche complete EDTA-free), and lysed by sonication. Lysates

2 were centrifuged (50,000 x g, 4°C, 1 h) and rSodA was purified from the soluble fraction by

3 fast protein liquid chromatography using a HisTrap column (GE Healthcare). rSodA was

4 eluted using a 25 to 500 mM imidazole gradient in buffer A, and imidazole was removed by

5 dialysis against buffer A using a 10,000 Da molecular weight cutoff membrane. The 6xHis

6 tag from rSodA was removed by digestion with TEV (44) at 4 °C overnight, followed by

7 passing the reaction through a HisTrap column and collecting the flowthrough. The identity

8 of tag-free rSodA (23.48 kDa) was confirmed by electrospray ionization mass spectrometry.

9 Protein concentration was estimated using absorbance at 280 nm with molar extinction

10 coefficient of 40,910 M^{-1} cm^{-1} (calculated using ExPASy (45)) as well as BCA assay

11 (Thermo Scientific).

12

13 **SOD activity assays**

14 To determine the role of metal ions in SOD activity, overnight cultures were inoculated to

15 OD_{600} = 0.025 in THY with or without Fe(II) or Mn(II). Strains were cultured to OD_{600} 0.6-

16 0.8, harvested by centrifugation (3,200 x g, 15 min, 4 °C), washed with HEPES buffer (50

17 mM, pH 7.4), resuspended in 1 mL of HEPES buffer (50 mM, pH 7.4), and lysed

18 mechanically on the FastPrep 120 instrument. For H_2O_2 challenge experiments, strains were

19 grown to OD_{600} = 0.6 and exposed to water (control) or H_2O_2 (1 or 4 mM) for 30 min. Cells

20 were harvested by centrifugation (3,200 x g, 15 min, 4 °C), washed with HEPES buffer (50

21 mM, pH 7.4), resuspended in 1 mL of HEPES buffer (50 mM, pH 7.4), and lysed

22 mechanically on the FastPrep 120 instrument.

23

24 GAS lysates were centrifuged (20,000 x g, 2 min) and soluble fractions were used in SOD

25 assay (Sigma-Aldrich) following manufacturers' instructions. Protein concentrations in the

1 lysates were determined using BCA assay (Thermo Scientific). Lysates were assayed for

2 SOD activity using a commercial SOD assay kit (Sigma-Aldrich) following manufacturers'

3 instructions.

4

5 Purified rSodA-Fe or rSodA-Mn were prepared in HEPES buffer (50 mM, pH 7.4) and

6 assessed for SOD activity using a commercial SOD assay kit (Sigma-Aldrich) following

7 manufacturers' instructions.

8

9 **SOD gel activity assays**

10 Whole cell lysates (40 µg) were resolved on native PAGE gels. Gels were incubated with

11 0.1% nitroblue tetrazolium (NBT) in deionised water for 1 h with gentle shaking, washed 3

12 times with water, and finally incubated with (-)-riboflavin (28 µM) in phosphate buffer (100

13 mM, pH 7) containing TEMED (28 mM) for 15 min in the dark with gentle shaking. Gels

14 were washed 3 more times with water and subsequently exposed to light to promote colour

15 development.

16

17 **Data analysis**

18 All data were analysed using GraphPad Prism 7. Analyses of ICP-MS and gene expression

19 data were performed using either 1-way ANOVA or 2-way ANOVA (for comparison of

20 strains under mixed conditions) as indicated. 2-way ANOVA was used to compare to either

21 the WT control of that treatment or to assess differences within strains as a result of

22 treatment, compared to H_2O as control. For 1-way or 2-way ANOVA, Tukey's or Dunnett's

23 post-hoc tests were used, respectively. Growth curve data represents mean ± standard

24 deviation of at least 4 independent biological replicates. SOD assays show mean ± standard

25 deviation of at least 4 independent biological replicates.

1   **Results**

2   **Mn is imported in response to hydrogen peroxide stress**

3   We previously demonstrated that PmtA is a PerR-regulated Fe export pump (28). Based on

4   these results, we hypothesised that intracellular Fe levels would fall in response to H_2O_2

5   shock as a consequence of PmtA activity. To determine changes in the intracellular metal

6   levels of GAS during oxidative stress, we cultured 5448 WT in THY medium to the mid-

7   exponential phase and subsequently exposed this culture to 0, 1, or 4 mM H_2O_2 for 30 min.

8   Surprisingly, treatment with high concentrations of H_2O_2 (4 mM) led to a 1.5-fold increase in

9   intracellular Fe levels, rather than the predicted decrease (Figure 1A), and this increase

10   occurred independently of changes in bacterial viability, as determined by CFU counts

11   (Figure S1).

12

13   To assess the role of PmtA in the H_2O_2-induced increase in intracellular Fe, we next

14   compared the levels of intracellular Fe in 5448 WT, 5448Δ*pmtA*, and 5448Δ*pmtA::pmtA*

15   complemented strains following H_2O_2 challenge. Consistent with our previous observations

16   (28), the 5448Δ*pmtA* strain accumulated 2.1-fold higher intracellular Fe levels when

17   compared to the isogenic parent and complemented strains (Figure 1B). Similar to the 5448

18   WT and 5448Δ*pmtA::pmtA* complemented mutant, the amounts of intracellular Fe in

19   5448Δ*pmtA* also increased following exposure to 4 mM H_2O_2 (Figure 1B). While these

20   results were consistent with our previous description of PmtA as an Fe efflux pump (28), they

21   did not identify the mechanism underpinning the observed increase in intracellular Fe in

22   response to oxidative stress (Figure 1A).

23

24   In addition to an increase in intracellular Fe levels, we detected a 3.7-fold increase in

25   intracellular Mn levels in the 5448 WT strain following exposure to as low as 1 mM H_2O_2

1   (Figure 1C). This increase also occurred in the 5448Δ*pmtA* strain but failed to reach levels

2   observed in the 5448 WT and 5448Δ*pmtA::pmtA* complemented strains under any condition

3   (Figure 1D). In fact, basal Mn levels in 5448Δ*pmtA* before exposure to H_2O_2 were

4   reproducibly lower than those in the WT or complemented mutant strains (Figure 1D), an

5   opposite phenotype to that observed for intracellular Fe levels (Fig 1B). Together, these

6   findings suggest that there might be coordinated shifts of intracellular Fe and Mn levels in

7   GAS, particularly during conditions of oxidative stress.

8

9   **Mn uptake during hydrogen peroxide stress requires MtsABC**

10   To determine whether the observed increase in intracellular Mn (Figure 1C) required the Mn

11   importer MtsABC, we constructed the 5448Δ*mtsABC* deletion and 5448Δ*mtsABC::mtsABC*

12   complemented mutant strains. As reported previously for M1 GAS (21), growth of

13   5448Δ*mtsABC* in THY was impaired, as evidenced by a prolonged doubling time (1.6 ± 0.2 h

14   for this mutant *vs.* 1.2 ± 0.1 h for 5448 WT) and a lower stationary phase optical density

15   compared to the wild type and complemented mutant strains (Figure 2A). This growth defect

16   was abolished by addition of 10 μM Mn(II) (Figure 2B) but not Fe(II) or Zn(II) (Figure S2).

17   Consistent with the role of MtsABC in Mn uptake, we found that 5448Δ*mtsABC* was Mn-

18   deficient when compared to the isogenic parent or the complemented mutant strains (Figure

19   2C). This deficiency was again alleviated by supplementing the culture medium with 20 μM

20   Mn(II) (Figure 2C), indicating that alternative low-affinity or non-specific Mn import

21   pathways may be present in GAS.

22

23   In contrast to Mn, levels of intracellular Fe in 5448Δ*mtsABC* were identical with those in the

24   wild type or the 5448Δ*mtsABC::mtsABC* complemented strains, regardless of whether they

25   were cultured in THY alone, in the presence of the Fe chelator 2,2'-bipyridyl (20 μM), or in

1   the presence of Fe(II) (20 μM, 200 μM, or 2 mM) (Figure 2D), indicating that MtsABC did

2   not facilitate Fe import under these experimental conditions.

3

4   We next examined the effects of oxidative stress on intracellular Mn levels in the

5   5448Δ*mtsABC* mutant. Unlike the 5448 WT or the 5448Δ*mtsABC::mtsABC* complemented

6   strains, intracellular Mn levels in 5448Δ*mtsABC* remained low (~8-fold less Mn compared

7   with 5448 WT and 5448Δ*mtsABC::mtsABC*) under all conditions. Exposure to 1 mM H_2O_2

8   did result in a 2-fold increase in intracellular Mn levels in the 5448Δ*mtsABC* mutant (Figure

9   2E) but this effect was not statistically significant. These results established that the influx of

10   Mn during conditions of oxidative stress was dependent on MtsABC. By contrast to Mn,

11   intracellular Fe levels in 5448Δ*mtsABC* were not significantly different from that of the

12   isogenic parent or complemented mutant strains (Figure 2F), again consistent with the

13   proposal that MtsABC does not facilitate import of Fe under these conditions.

14

15   **Hydrogen peroxide stress does not induce the expression of *mtsABC***

16   The transcriptional response to oxidative stress in GAS is controlled by the H_2O_2-sensing

17   transcriptional regulator PerR. However, a recent study in *S. cristatus* showed that the MtsR

18   homologue MntR is also a H_2O_2 sensor (37). Hence, we hypothesised that the observed

19   increase in intracellular Mn (Figure 1C) occurred following transcriptional upregulation of

20   MtsABC, either by MtsR or PerR, or both. To test this proposal, we examined the levels of

21   *mtsA* mRNA in the 5448Δ*mtsR* and 5448Δ*perR* mutant and complemented strains, as well as

22   the 5448Δ*mtsABC* mutant and its complemented strains in response to H_2O_2, using the same

23   experimental conditions as in Figure 1 (Figure 3).

24

1　　As shown in Figure 3A, deletion of *mtsR* led to the constitutive upregulation of *mtsA*

2　　regardless of the experimental condition, consistent with MtsR acting as a transcriptional

3　　repressor of *mtsABC*. As anticipated, other known MtsR-regulated genes such as *shp, shr*,

4　　and *siaA* were also constitutively upregulated (Figure S3A-C). In comparison, expression of

5　　*pmtA*, which is not regulated by MtsR, did not change in an MtsR-dependent manner (Figure

6　　S3D). We further confirmed that transcription of *mtsA* was Mn-responsive and showed that

7　　addition of Mn(II) led to downregulation of *mtsA* expression in the 5448 WT strain (Figure

8　　3A), consistent with repression by Mn-MtsR. In contrast, expression of *mtsA* remained

9　　unchanged in the 5448Δ*perR* mutant (Figure 3B). Under the same conditions, deletion of

10　　*perR* led to the constitutive upregulation of known PerR-regulated genes *pmtA*, *ahpC*, and

11　　*dpr* (Figure S4A-C). Together, these results indicated that *mtsA* is not part of the PerR

12　　regulon in GAS. Consistent with this finding, there is no Per box upstream of the *mtsABC*

13　　operon in GAS (26).

14

15　　Consistent with the idea that PerR is not involved in the regulation of *mtsABC*, we detected a

16　　2-fold decrease in *mtsA* expression, albeit not statistically significant, in the 5448 WT and

17　　5448Δ*mtsABC::mtsABC* complemented strains following challenge with 1 mM H_2O_2 and a

18　　statistically significant decrease (~5-fold) upon treatment with 4 mM H_2O_2 (Figure 3C).

19　　Transcription of *mtsA* in the 5448Δ*pmtA* mutant mirrored this trend (Figure S5A). In

20　　comparison, the PerR-regulated genes *pmtA*, *dpr*, *ahpF,* and *sodA* were all upregulated by

21　　H_2O_2 (Figure S5C-J), the opposite trend from *mtsA*. This downregulation of *mtsA* expression

22　　occurred as early as 5 minutes post-exposure to H_2O_2 (Figure 3D), whereas PerR-regulated

23　　genes *dpr*, *sodA,* and *ahpF* were all upregulated within the same time period (Figure S6A-C).

24　　Therefore, although the increase in intracellular Mn during oxidative stress required a

1 functional MtsABC transporter (Figure 2E), it did not appear to involve transcriptional

2 upregulation of *mtsABC* by MtsR.

3

4 **Exposure to hydrogen peroxide stimulates SOD activity and this process requires**

5 **MtsABC**

6 Having shown that exposure to H_2O_2 led to MtsABC-dependent uptake of Mn (Figure 2E)

7 and increased transcription of *sodA* (Figure S5I-J), we next determined whether the

8 intracellular accumulation of Mn led to an increase in SodA enzyme activity. Following a

9 short (30 min) exposure to 1 mM H_2O_2, we detected a ~3-fold increase in SodA activity in

10 the 5448 WT strain (Figure 4A and Figure S7A). This result was consistent with the expected

11 role of SodA activity in protecting the cell during conditions of oxidative stress (46). As a

12 control, we confirmed that there was negligible superoxide dismutase activity in the

13 5448Δ*sodA* strain, regardless of H_2O_2 exposure (Figure 4A and Figure S7A).

14

15 To determine whether the H_2O_2-mediated increase in SodA activity was dependent on the

16 import of Mn *via* MtsABC, we repeated the above experiment using the 5448Δ*mtsABC*

17 mutant strain (Figure 2C). We noted that basal activity of SodA in 5448Δ*mtsABC*, even

18 before exposure to H_2O_2, was reproducibly lower when compared with the 5448 WT and

19 5448Δ*mtsABC*∷*mtsABC* complemented strains (Figure 4A and Figure S7A), consistent with

20 previously reported findings (21). SodA activity was restored to wild type levels by addition

21 of exogenous Mn(II) (40 µM) (Figure 4B and Figure S7B), mirroring the finding that Mn

22 deficiency in the 5448Δ*mtsABC* mutant was corrected by addition of Mn salts (Figure 2C).

23 Importantly, Mn supplementation did not affect background activity in the 5448Δ*sodA*

24 mutant (Figure S7B), indicating that any potential contribution from non-SodA Mn-protein or

25 Mn-sugar complexes in superoxide quenching was negligible (47, 48).

1

2   Following treatment with 1 mM H_2O_2, amounts of *sodA* mRNA in 5448Δ*mtsABC* increased

3   to levels that were comparable with those in the isogenic parent and complemented strains

4   (Figure S5J). However, unlike 5448 WT and 5448Δ*mtsABC::mtsABC*, the increased

5   expression of *sodA* in 5448Δ*mtsABC* was only accompanied by a moderate, 1.5-fold increase

6   in SodA activity (Figure 4A). As shown in Figure 2E, this mutant accumulated lower

7   intracellular Mn during conditions of oxidative stress. Thus, it was likely that some of the

8   SodA enzymes in this mutant was produced in the *apo-* or incorrectly metalated form (20).

9   Consistent with this view, growth curve analysis indicated that while all strains displayed

10   identical growth in THY alone (Figure 4C), the 5448Δ*mtsABC* mutant was unable to grow in

11   the presence of the superoxide generator paraquat (1 mM) (Figure 4D). Nevertheless, growth

12   of this mutant was restored to wild type levels upon supplementation of the growth medium

13   with 10 μM Mn(II) (Figure 4E). As a control, 5448Δ*sodA* was unable to grow in the presence

14   of 1 mM paraquat, regardless of Mn supplementation. Together, these results indicated that

15   MtsABC is required for optimal metalation of SodA with Mn but supplemental Mn may be

16   imported *via* alternative transporters and become available to SodA. This corroborates

17   previous findings in GAS (21) and *Streptococcus gordonii* (49).

18

19   **SodA is less active in the Fe-metallated form**

20   We were surprised to find that SodA in the 5448 WT and 5448Δ*mtsABC::mtsABC*

21   complemented strains failed to activate upon exposure to 4 mM of H_2O_2 when compared with

22   1 mM H_2O_2 (Figure 4A), despite similar increases in *sodA* expression under these conditions

23   (Figure S5J). As shown in Figure 1D and Figure 2E, Mn was imported under both conditions.

24   However, the relative intracellular levels of Fe were higher upon exposure to 4 mM H_2O_2

25   compared with 1 mM H_2O_2 (Figures 2E and 2F). We therefore hypothesised that the

1 increased relative abundance of intracellular Fe might outcompete Mn from SodA, leading to

2 formation of Fe-SodA, and that the Fe-SodA form was less active than Mn-SodA.

3

4 To investigate the metal dependence of SodA, we purified recombinant GAS SodA from *E.*

5 *coli*. As we were unable to generate an *apo*-form of the enzyme for subsequent reconstitution

6 with only Mn or Fe, we prepared Mn- or Fe-metalated forms of SodA from *E. coli* cultured in

7 the presence of excess Fe(II) or Mn(II) salts (250 μM). ICP-MS analyses indicated that SodA

8 isolated from Mn-supplemented *E. coli* cultures contained 1.2 ± 0.2 (SD) molar equivalents

9 of Mn. This Mn-SodA form was relatively pure and it contained only 0.06 ± 0.08 (SD) molar

10 equivalents of contaminating Fe (Figure 5A). Conversely, SodA isolated from Fe-

11 supplemented *E. coli* cultures contained 0.8 ± 0.1 (SD) molar equivalents of Fe and 0.2 ± 0.0

12 (SD) molar equivalents of Mn (Figure 5A). We were unable to remove the Mn-SodA

13 contaminant from this mixture and so the enzyme was used as isolated. Subsequent

14 measurements of SodA activity of both the Mn- and the Fe- forms demonstrated that the Mn-

15 SodA displayed approximately four times as much activity as the Fe-SodA (Figure 5B).

16 Some of the activity in the Fe-SodA sample may be attributed to Mn-SodA contamination,

17 but nonetheless our results support our proposal that Fe-SodA was less active than Mn-SodA.

18 Hence, we propose that GAS SodA may be a cambialistic enzyme, similar to SodM from

19 *Staphylococcus aureus* (23), though the GAS SodA appeared to displays less activity with Fe

20 as a cofactor.

21

22 **PmtA protects SodA from mis-metalation by Fe**

23 We have previously shown that the 5448Δ*pmtA* mutant was sensitive to the superoxide

24 generator paraquat (28). As shown in Figures 1B and 1D, 5448Δ*pmtA* displayed a higher

25 intracellular Fe/Mn ratio when compared with the WT or complemented strains. We therefore

1 hypothesised that the excess intracellular Fe may promote the Fenton reaction in the presence

2 of paraquat, whilst Mn might quench this reactive oxygen species (28). As described

3 previously (28), growth curve analysis showed that in THY alone, all strains grew equally

4 well (Figure 6A), but the addition of 2 mM paraquat resulted in diminished growth of the

5 5448Δ*pmtA* mutant (Figure 6B) and we were able to rescue growth by adding excess Mn(II)

6 into the growth medium (Figure 6C).

7

8 Our experiments with recombinant SodA indicated that excess intracellular Fe may lead to

9 mis-metalation of SodA, leading to generation of the less active Fe-SodA enzyme. To test

10 this proposal, we first examined the effects of excess exogenous Fe(II) on SodA activity in

11 the 5448 WT strains. As anticipated, we found that Fe treatment led to a complete loss of

12 SodA activity to background levels (*i.e.* levels in 5448Δ*sodA* mutant strain) (Figure 6D and

13 Figure S7). This reduction in SodA activity may arise from downregulation of *sodA* by Fe(II)

14 but there was only a small decrease (1.5-fold) in *sodA* gene expression under the same

15 conditions (Figure S9). As a control, we also measured SodA activity in 5448 WT cultures in

16 the presence of excess exogenous Mn(II). As anticipated, we observed an increase in SodA

17 activity in 5448 WT but not in 5448Δ*sodA* mutant (Figure 6D and Figure S7C). Thus, our

18 results indicated that the loss of SodA activity likely occurred from the incorporation of Fe

19 into the enzyme.

20

21 In the 5448Δ*pmtA* mutant strain, which was Fe-rich and Mn-deficient, we detected a lower

22 basal SodA activity when compared to the 5448 WT and 5448Δ*pmtA::pmtA* complemented

23 strains (Figure 6D-E and Figure S7C-D). Although exposure of 5448Δ*pmtA* to 1 mM H_2O_2

24 upregulated transcription of *sodA* to levels that were comparable to those in the isogenic

25 parent or complemented mutant strains (Figure S5I), SodA activity in 5448Δ*pmtA* reached

1 only half of that in 5448 WT and 5448Δ*pmtA::pmtA* (Figure 6E and Figure S7D). These

2 trends were mirrored by SOD in-gel activity assays (Figure S8). Under these conditions of

3 oxidative stress, we found that 5448Δ*pmtA* accumulated more Fe (Figure 1B) and less Mn

4 (Figure 1D) than did the 5448 WT parent strain. Thus, our findings were again consistent

5 with the suggestion that SodA may be partially metalated with Fe and that the Fe-SodA form

6 was less active than Mn-SodA.

7

8 **MtsR is critical for Mn and Fe homeostasis during oxidative stress**

9 Although it is established that MtsR differentially controls expression of Mn uptake genes

10 (*mtsABC*) and Fe uptake genes (*shp*, *shr*, and *siaA*) (Figure 3A, Figure S3A-C), its role in

11 regulating the balance of Mn and Fe inside cells is not fully understood. Given the

12 constitutive upregulation of *mtsA* in a 5448Δ*mtsR* mutant, we anticipated that this strain

13 would accumulate Mn. Contrary to this hypothesis, 5448Δ*mtsR* was Mn-deficient compared

14 to 5448 WT and 5448Δ*mtsR::mtsR* (Figure 7A). Instead of Mn, 5448Δ*mtsR* appeared to

15 accumulate Fe (Figure 7A) and, consistent with this observation, 5448Δ*mtsR* was unable to

16 grow in the presence of the Fe-dependent antibiotic streptonigrin (Figure 7B). These results

17 can be explained by the constitutive upregulation of Fe uptake genes *shp*, *shr*, and *siaA* in

18 5448Δ*mtsR*.

19

20 The Fe-rich and Mn-deficient phenotype of 5448Δ*mtsR* was reminiscent of 5448Δ*pmtA*

21 (Figure 1B and 1D) but the underlying mechanism was likely different. The MtsR-regulated

22 Fe uptake gene *shp* was not upregulated in 5448Δ*pmtA* when compared with the isogenic

23 parent or complemented strains (Figure S5K). Hence, the increase in intracellular Fe in

24 5448Δ*pmtA* was not a consequence of Fe influx *via* MtsR-dependent Fe uptake systems, but

25 rather was attributed to the loss of PmtA and the inability to remove excess Fe. Similarly,

1 basal expression levels of *mtsA* in 5448Δ*pmtA* were largely unchanged when compared with

2 those in the WT or complemented mutant strains (Figure 7C). Thus, the observed Mn

3 deficiency was not related to a loss of MtsABC expression. Nevertheless, addition of 2 mM

4 Fe(II) to 5448Δ*pmtA* did result in a 28-fold downregulation of *mtsA* (Figure 7C). We

5 hypothesise that the excess intracellular Fe in 5448Δ*pmtA* may lead to formation of Fe-MtsR

6 and constitutive repression of *mtsA*. To date, the precise binding affinities of MtsR for Mn

7 and Fe and their respective affinities (and/or allosteric free energies) to the *mtsA*, *sia*, *shp*,

8 and *shr* promoters are unknown and warrant future investigation.

9

10 In the case of 5448Δ*perR*, we found that this mutant contained less Fe but more Mn relative

11 to 5448 WT and 5448Δ*perR::perR* (Figure 7D). The Fe-deficient phenotype was consistent

12 with constitutive upregulation of the Fe efflux pump *pmtA* (Figure S4A) (26, 28). This

13 mutant was reproducibly less sensitive to streptonigrin when compared to the parent or the

14 complemented mutant strains (Figure 7B). The Mn-rich phenotype was also reported

15 previously for the Δ*perR* mutant of *S. cristatus* (50) but it could not be explained by our

16 current understanding of PerR regulation, particularly considering the lack of a Per box

17 upstream of *mtsABC* (50) and our findings that *mtsA* was not constitutively activated in

18 5448Δ*perR* (Figure 3B).

19

20 **DISCUSSION**

21 It is now established that during host-pathogen interactions, systemic and niche-specific Mn

22 levels in the host are kept low by Mn-sequestering host effectors such as calprotectin (51,

23 52). Conversely, high-affinity uptake systems for Mn are known to be important for the

24 virulence of a number of pathogenic bacteria, including PsaABC in *S. pneumoniae* (53, 54)

25 and MtsABC in GAS (21). Nonetheless, we have previously shown that excess Mn can be

1   toxic to GAS and that this bacterium requires the cation diffusion facilitator, MntE, to efflux

2   excess Mn (40). Our work herein describes the complementary roles of the Mn importer

3   MtsABC and the Fe efflux pump PmtA in GAS Fe/Mn metal homeostasis and their

4   contribution to oxidative stress defence, particularly in ensuring optimal metalation of SodA

5   (Figure 8A). Our data also suggest an interplay or overlapping roles between MtsR and PerR

6   in Fe and Mn homeostasis in GAS but several outstanding questions remain.

7

8   One surprising result from this study is the observation that, while the increase in intracellular

9   Mn in response to H_2O_2 required a functional MtsABC, the levels of *mtsABC* expression

10   decreased (instead of increased) under oxidative stress conditions (Figure 3C). A potential

11   rationalisation of this observation is that MtsABC activity increases in response to H_2O_2

12   stress. Our data demonstrated that GAS has a relatively high intracellular Fe/Mn ratio when

13   grown in THY. This ratio mirrored the relative metal composition of THY, which contained

14   15.6 ± 0.7 μM Fe and 0.30 ± 0.01 μM Mn. We propose that extracellular Fe (in the Fe(II)

15   form) in THY may compete for the Mn(II) binding site in MtsA (the solute-binding protein)

16   and subsequently inhibit Mn(II) import during normal conditions (Figure 8A). Consistent

17   with this idea, intracellular Mn levels did not increase in the 5448Δ*mtsR* mutant, despite

18   constitutive upregulation of *mtsABC*. However, addition of H_2O_2 into the culture medium (to

19   enforce conditions of oxidative stress) may lead to oxidation of extracellular Fe(II) to Fe(III)

20   and subsequent dissociation of Fe(III) from MtsA, allowing Mn import to occur. There was

21   also a hint that excess intracellular Fe may block Mn uptake *via* MtsABC, with 5448Δ*pmtA*

22   showing decreased intracellular Mn levels when compared with 5448 WT and

23   5448Δ*pmtA::pmtA* despite comparable levels of *mtsA* expression (Figure 7C, 8B). Whether

24   the excess cytoplasmic Fe blocks Mn import by binding to the cytoplasmic domains of

25   MtsABC and/or locking this transporter in a closed or non-functional state is unknown.

1

2   The Mn-rich phenotype of the 5448Δ*perR* mutant also requires further investigation.

3   Previous microarray data reported that the *mts* operon was downregulated in a Δ*perR* mutant

4   of the M1 strain AP1 (26). By contrast, deletion of *perR* in the M3 strain 003Sm (55) or the

5   M14 strain HSC5 (56) did not appear to affect *mts* transcription. Furthermore, in M1T1

6   MGAS5005 *perR* mutant, *mtsA* was found to be upregulated (31) but this experiment used

7   metal-depleted THY medium, which may have provided different growth conditions

8   compared to that used in the present study. Nonetheless, the pattern of regulation of *mtsA* in

9   response to Fe and Mn that we observed is consistent with other published findings (31). In

10   the 5448Δ*perR* mutant, the constitutive activation of *pmtA* and subsequent Fe efflux leads to

11   low intracellular Fe. As a consequence, MtsR may sense these low Fe levels and activate

12   MtsR-regulated genes including *mtsABC*. The import of Fe by Sia and Siu (57) may result in

13   cycling of Fe but at the same time permit Mn to accumulate inside the cytoplasm due to

14   activation of MtsABC (21).

15

16   An additional key question that arises relates to the mechanism of differential regulation of

17   Mn uptake genes (*mtsABC*) and Fe uptake genes (*shp*, *shr*, *siaA*) by MtsR (Figure 3A and

18   Figure S3). Previous work with MtsR from MGAS5005 indicated that the Mn- and Fe-forms

19   of MtsR display distinct affinities for DNA. Mn-MtsR was shown to bind with high affinity

20   to the *mtsABC* promoter, while Fe-MtsR exhibited a lower affinity to the same sequence. In

21   addition, Mn-MtsR bound with high affinity to the *sia* and *siu* promoters but exhibited low

22   affinity binding to the *siu* promoter in the presence of Fe. (31). In this work, we showed that,

23   unlike *mtsA*, expression of *shp* appeared to increase (instead of decrease) in response to 4

24   mM H_2O_2. Even though MtsR from GAS and MntR from *S. cristatus* share high amino acid

25   sequence identity (98% cover, 55% identity, $2x10^{-87}$ E-value), including the H_2O_2-sensing

1 cysteine residues Cys11 and Cys123, H_2O_2 did not induce expression of *mtsA* in GAS as

2 shown for *S. cristatus* (37). GAS MtsR lacks the Cys156 residue present in *S. cristatus* MntR.

3 Cys156 has been shown to play a role in disulfide bond formation in response to H_2O_2 stress

4 (37), and so its absence in GAS MtsR may explain the lack of H_2O_2-dependent gene

5 expression of *mtsA* at low levels of H_2O_2. Thus, GAS appears to use both MtsR and PerR to

6 control Fe homeostasis. Given the differing requirements of GAS for Fe and Mn, and the

7 opposing effects of these two metal ions on SodA activity and the response to oxidative

8 stress, the mechanisms for how Fe and Mn homeostasis are organised or coordinated

9 represent an interesting topic for future studies.

10

25

1 **Author contribution statement**

2 AGT, KYD, CYO, MJW, and AGM conceived the project and designed experiments. AGT

3 performed experimentation. TCB provided reagents and critiqued experimental design. AGT,

4 KYD, CYO, MJW, and AGM wrote the manuscript and all authors edited the manuscript.

5

6 **References**

7 1.   Skaar EP, Raffatellu M. Metals in infectious diseases and nutritional immunity.

8 Metallomics : integrated biometal science. 2015;7(6):926-8.

9 2.   Kehl-Fie TE, Skaar EP. Nutritional immunity beyond iron: a role for manganese and

10 zinc. Curr Opin Chem Biol. 2010;14(2):218-24.

11 3.   Achard ME, Stafford SL, Bokil NJ, Chartres J, Bernhardt PV, Schembri MA, et al.

12 Copper redistribution in murine macrophages in response to *Salmonella* infection. Biochem J.

13 2012;444(1):51-7.

14 4.   Kapetanovic R, Bokil NJ, Achard ME, Ong CL, Peters KM, Stocks CJ, et al.

15 *Salmonella* employs multiple mechanisms to subvert the TLR-inducible zinc-mediated

16 antimicrobial response of human macrophages. FASEB J. 2016;30(5):1901-12.

17 5.   Shah S, Dalecki AG, Malalasekera AP, Crawford CL, Michalek SM, Kutsch O, et al.

18 8-Hydroxyquinolines are boosting-agents of copper related toxicity in *Mycobacterium*

19 *tuberculosis*. Antimicrob Agents Chemother. 2016;60(10):5765-76.

20 6.   Botella H, Peyron P, Levillain F, Poincloux R, Poquet Y, Brandli I, et al.

21 Mycobacterial P_1-type ATPases mediate resistance to zinc poisoning in human macrophages.

22 Cell Host Microbe. 2011;10(3):248-59.

23 7.   Ong CL, Gillen CM, Barnett TC, Walker MJ, McEwan AG. An antimicrobial role for

24 zinc in innate immune defense against Group A *Streptococcus*. J Infect Dis.

25 2014;209(10):1500-8.

1 8.   Fang FC. Antimicrobial reactive oxygen and nitrogen species: concepts and

2 controversies. Nat Rev Microbiol. 2004;2(10):820-32.

3 9.   Valko M, Morris H, Cronin MTD. Metals, toxicity and oxidative stress. Curr Med

4 Chem. 2005;12(10):1161-208.

5 10.   Horsburgh MJ, Wharton SJ, Karavolos M, Foster SJ. Manganese: elemental defence

6 for a life with oxygen? Trends Microbiol. 2002;10(11):496-501.

7 11.   Juttukonda LJ, Skaar EP. Manganese homeostasis and utilization in pathogenic

8 bacteria. Mol Microbiol. 2015;97(2):216-28.

9 12.   Walker MJ, Barnett TC, McArthur JD, Cole JN, Gillen CM, Henningham A, et al.

10 Disease manifestations and pathogenic mechanisms of Group A *Streptococcus*. Clin

11 Microbiol Rev. 2014;27(2):264-301.

12 13.   Kwinn LA, Nizet V. How Group A *Streptococcus* circumvents host phagocyte

13 defenses. Future Microbiol. 2007;2(1):75-84.

14 14.   Fieber C, Kovarik P. Responses of innate immune cells to Group A *Streptococcus*.

15 Front Cell Infect Microbiol. 2014;4:140.

16 15.   Cole JN, Barnett TC, Nizet V, Walker MJ. Molecular insight into invasive group A

17 streptococcal disease. Nat Rev Microbiol. 2011;9(10):724-36.

18 16.   Turner AG, Ong C-lY, Walker MJ, Djoko KY, McEwan AG. Transition metal

19 homeostasis in *Streptococcus pyogenes* and *Streptococcus pneumoniae*. In: Robert KP,

20 editor. Adv Microb Physiol. Volume 70: Academic Press; 2017. p. 123-91.

21 17.   King KY, Horenstein JA, Caparon MG. Aerotolerance and peroxide resistance in

22 peroxidase and PerR mutants of *Streptococcus pyogenes*. J Bacteriol. 2000;182(19):5290-9.

23 18.   Henningham A, Dohrmann S, Nizet V, Cole JN. Mechanisms of group A

24 *Streptococcus* resistance to reactive oxygen species. FEMS Microbiol Rev. 2015;39:488-508.

1   19.   Brenot A, King KY, Janowiak B, Griffith O, Caparon MG. Contribution of

2   glutathione peroxidase to the virulence of *Streptococcus pyogenes*. Infect Immun.

3   2004;72(1):408-13.

4   20.   Gerlach D, Reichardt W, Vettermann S. Extracellular superoxide dismutase from

5   *Streptococcus pyogenes* type 12 strain is manganese-dependent. FEMS Microbiol Lett.

6   1998;160(2):217-24.

7   21.   Janulczyk R, Ricci S, Bjorck L. MtsABC is important for manganese and iron

8   transport, oxidative stress resistance, and virulence of *Streptococcus pyogenes*. Infect Immun.

9   2003;71(5):2656-64.

10   22.   Eijkelkamp BA, Morey JR, Ween MP, Ong CL, McEwan AG, Paton JC, et al.

11   Extracellular zinc competitively inhibits manganese uptake and compromises oxidative stress

12   management in *Streptococcus pneumoniae*. PLoS One. 2014;9(2):e89427.

13   23.   Garcia YM, Barwinska-Sendra A, Tarrant E, Skaar EP, Waldron KJ, Kehl-Fie TE. A

14   superoxide dismutase capable of functioning with iron or manganese promotes the resistance

15   of *Staphylococcus aureus* to calprotectin and nutritional immunity. PLoS Pathogens.

16   2017;13(1).

17   24.   Brenot A, King KY, Caparon MG. The PerR regulon in peroxide resistance and

18   virulence of *Streptococcus pyogenes*. Mol Microbiol. 2005;55(1):221-34.

19   25.   Grifantini R, Toukoki C, Colaprico A, Gryllos I. Peroxide stimulon and role of PerR

20   in Group A *Streptococcus*. J Bacteriol. 2011;193(23):6539-51.

21   26.   Ricci S, Janulczyk R, Bjorck L. The regulator PerR is involved in oxidative stress

22   response and iron homeostasis and is necessary for full virulence of *Streptococcus pyogenes*.

23   Infect Immun. 2002;70(9):4968-76.

24   27.   Lee JW, Helmann JD. The PerR transcription factor senses H_2O_2 by metal-catalysed

25   histidine oxidation. Nature. 2006;440(7082):363-7.

1   28.   Turner AG, Ong C-lY, Djoko KY, West NP, Davies MR, McEwan AG, et al. The

2   PerR-regulated P_{1B-4}-type ATPase (PmtA) acts as a ferrous iron efflux pump in *Streptococcus*

3   *pyogenes*. Infect Immun. 2017;85(6).

4   29.   VanderWal AR, Makthal N, Pinochet-Barros A, Helmann JD, Olsen RJ,

5   Kumaraswami M. Iron efflux by PmtA is critical for oxidative stress resistance and

6   contributes significantly to group A *Streptococcus* virulence. Infect Immun. 2017;85(6).

7   30.   Makthal N, Rastegari S, Sanson M, Ma Z, Olsen RJ, Helmann JD, et al. Crystal

8   structure of peroxide stress regulator from *Streptococcus pyogenes* provides functional

9   insights into the mechanism of oxidative stress sensing. J Biol Chem. 2013;288(25):18311-

10   24.

11   31.   Hanks TS, Liu MY, McClure MJ, Fukumura M, Duffy A, Lei BF. Differential

12   regulation of iron- and manganese-specific MtsABC and heme-specific HtsABC transporters

13   by the metalloregulator MtsR of Group A *Streptococcus*. Infect Immun. 2006;74(9):5132-9.

14   32.   Montanez GE, Neely MN, Eichenbaum Z. The streptococcal iron uptake (Siu)

15   transporter is required for iron uptake and virulence in a zebrafish infection model.

16   Microbiol-Sgm. 2005;151:3749-57.

17   33.   Hanks TS, Liu M, McClure MJ, Lei B. ABC transporter FtsABCD of *Streptococcus*

18   *pyogenes* mediates uptake of ferric ferrichrome. BMC Microbiol. 2005;5:62.

19   34.   Bates CS, Montanez GE, Woods CR, Vincent RM, Eichenbaum Z. Identification and

20   characterization of a *Streptococcus pyogenes* operon involved in binding of hemoproteins and

21   acquisition of iron. Infect Immun. 2003;71(3):1042-55.

22   35.   Sook BR, Block DR, Sumithran S, Montanez GE, Rodgers KR, Dawson JH, et al.

23   Characterization of SiaA, a streptococcal heme-binding protein associated with a heme ABC

24   transport system. Biochemistry. 2008;47(8):2678-88.

1   36.   Akbas N, Draganova EB, Block DR, Sook BR, Chan YF, Zhuo J, et al. Heme-bound

2   SiaA from *Streptococcus pyogenes*: Effects of mutations and oxidation state on protein

3   stability. J Inorg Biochem. 2016;158:99-109.

4   37.   Chen ZY, Wang XH, Yang F, Hu QQ, Tong HC, Dong XZ. Molecular insights into

5   hydrogen peroxide-sensing mechanism of the metalloregulator MntR in controlling bacterial

6   resistance to oxidative stresses. J Biol Chem. 2017;292(13):5519-31.

7   38.   Chatellier S, Ihendyane N, Kansal RG, Khambaty F, Basma H, Norrby-Teglund A, et

8   al. Genetic relatedness and superantigen expression in group A *Streptococcus* serotype M1

9   isolates from patients with severe and nonsevere invasive diseases. Infect Immun.

10   2000;68(6):3523-34.

11   39.   Bertani G. Studies on lysogenesis. I. The mode of phage liberation by lysogenic

12   *Escherichia coli*. J Bacteriol. 1951;62(3):293-300.

13   40.   Turner AG, Ong CL, Gillen CM, Davies MR, West NP, McEwan AG, et al.

14   Manganese homeostasis in Group A *Streptococcus* is critical for resistance to oxidative stress

15   and virulence. mBio. 2015;6(2):e00278-15.

16   41.   Venturini C, Ong CIY, Gillen CM, Ben-Zakour NL, Maamary PG, Nizet V, et al.

17   Acquisition of the Sda1-encoding bacteriophage does not enhance virulence of the serotype

18   M1 *Streptococcus pyogenes* strain SF370. Infect Immun. 2013;81(6):2062-9.

19   42.   Ramakers C, Ruijter JM, Deprez RH, Moorman AF. Assumption-free analysis of

20   quantitative real-time polymerase chain reaction (PCR) data. Neurosci Lett. 2003;339(1):62-

21   6.

22   43.   Livak KJ, Schmittgen TD. Analysis of relative gene expression data using real-time

23   quantitative PCR and the $2^{(-\Delta\Delta CT)}$ method. Methods. 2001;25(4):402-8.

1 44.   Kapust RB, Tozser J, Fox JD, Anderson DE, Cherry S, Copeland TD, et al. Tobacco

2 etch virus protease: mechanism of autolysis and rational design of stable mutants with wild-

3 type catalytic proficiency. Protein Eng. 2001;14(12):993-1000.

4 45.   Gasteiger E, Hoogland C, Gattiker A, Duvaud Se, Wilkins MR, Appel RD, et al.

5 Protein Identification and Analysis Tools on the ExPASy Server. In: Walker JM, editor. The

6 Proteomics Protocols Handbook. Totowa, NJ: Humana Press; 2005. p. 571-607.

7 46.   Miller AF. Superoxide dismutases: ancient enzymes and new insights. FEBS Lett.

8 2012;586(5):585-95.

9 47.   Archibald FS, Fridovich I. The scavenging of superoxide radical by manganous

10 complexes - *in vitro*. Arch Biochem Biophys. 1982;214(2):452-63.

11 48.   Al-Maghrebi M, Fridovich I, Benov L. Manganese supplementation relieves the

12 phenotypic deficits seen in superoxide-dismutase-null *Escherichia coli*. Arch Biochem

13 Biophys. 2002;402(1):104-9.

14 49.   Jakubovics NS, Smith AW, Jenkinson HF. Oxidative stress tolerance is manganese

15 Mn^{2+} regulated in *Streptococcus gordonii*. Microbiology. 2002;148(Pt 10):3255-63.

16 50.   Wang CH, Chuan CN, Kuo HT, Zheng PX, Tsou CC, Wang SY, et al. Peroxide

17 responsive regulator PerR of Group A *Streptococcus* is required for the expression of phage-

18 associated DNase Sda1 under oxidative stress. PLoS One. 2013;8(12):e81882.

19 51.   Hood MI, Skaar EP. Nutritional immunity: transition metals at the pathogen-host

20 interface. Nat Rev Microbiol. 2012;10(8):525-37.

21 52.   Kehres DG, Maguire ME. Emerging themes in manganese transport, biochemistry

22 and pathogenesis in bacteria. FEMS Microbiol Rev. 2003;27(2-3):263-90.

23 53.   Marra A, Lawson S, Asundi JS, Brigham D, Hromockyj AE. In vivo characterization

24 of the *psa* genes from *Streptococcus pneumoniae* in multiple models of infection.

25 Microbiology. 2002;148(Pt 5):1483-91.

1   54.   Tseng HJ, McEwan AG, Paton JC, Jennings MP. Virulence of *Streptococcus*

2   *pneumoniae*: PsaA mutants are hypersensitive to oxidative stress. Infect Immun.

3   2002;70(3):1635-9.

4   55.   Gryllos I, Grifantini R, Colaprico A, Cary ME, Hakansson A, Carey DW, et al. PerR

5   confers phagocytic killing resistance and allows pharyngeal colonization by Group A

6   *Streptococcus*. PLoS Pathogens. 2008;4(9):e1000145.

7   56.   Brenot A, Weston BF, Caparon MG. A PerR-regulated metal transporter (PmtA) is an

8   interface between oxidative stress and metal homeostasis in *Streptococcus pyogenes*. Mol

9   Microbiol. 2007;63(4):1185-96.

10   57.   Ge R, Sun X. Iron acquisition and regulation systems in *Streptococcus* species.

11   Metallomics : integrated biometal science. 2014;6(5):996-1003.

12

13

1
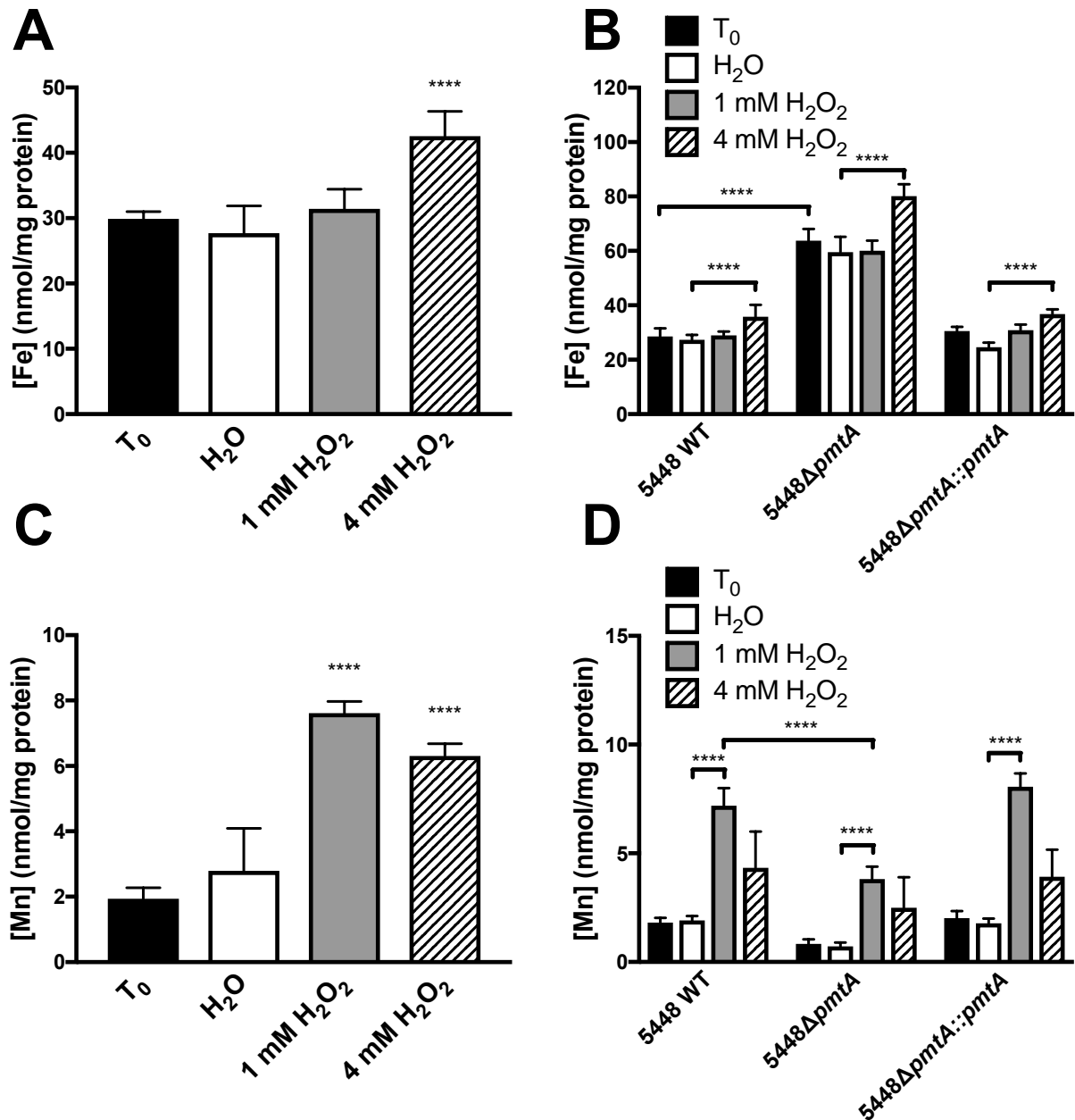
Figure 1 - Metal accumulation in GAS in response to oxidative stress

5448 WT was grown in THY at 37 °C to mid-exponential phase (OD_{600} 0.6 – 0.8) and

challenged with H_2O, or with 1 mM or 4 mM H_2O_2, and total intracellular accumulation of Fe

(**A**) or Mn (**C**) was assessed by ICP-MS. Strains 5448 WT, 5448$\Delta pmtA$ and

5448$\Delta pmtA::pmtA$ were grown in THY at 37 °C to mid-exponential phase (OD_{600} 0.6 – 0.8)

and challenged with H_2O, or with 1 mM or 4 mM H_2O_2, and total intracellular accumulation

of Fe (**B**) or Mn (**D**) was measured by ICP-MS. Total metal content was normalised to

1   protein content of the sample. Graph represents mean + standard deviation of 4 independent

2   biological replicates (1-way ANOVA comparing all samples to H_2O control and (2-way

3   ANOVA comparing strains to WT of that treatment or change due to treatment within strain,

4   compared to H_2O as control, **** $P < 0.0001$).

5
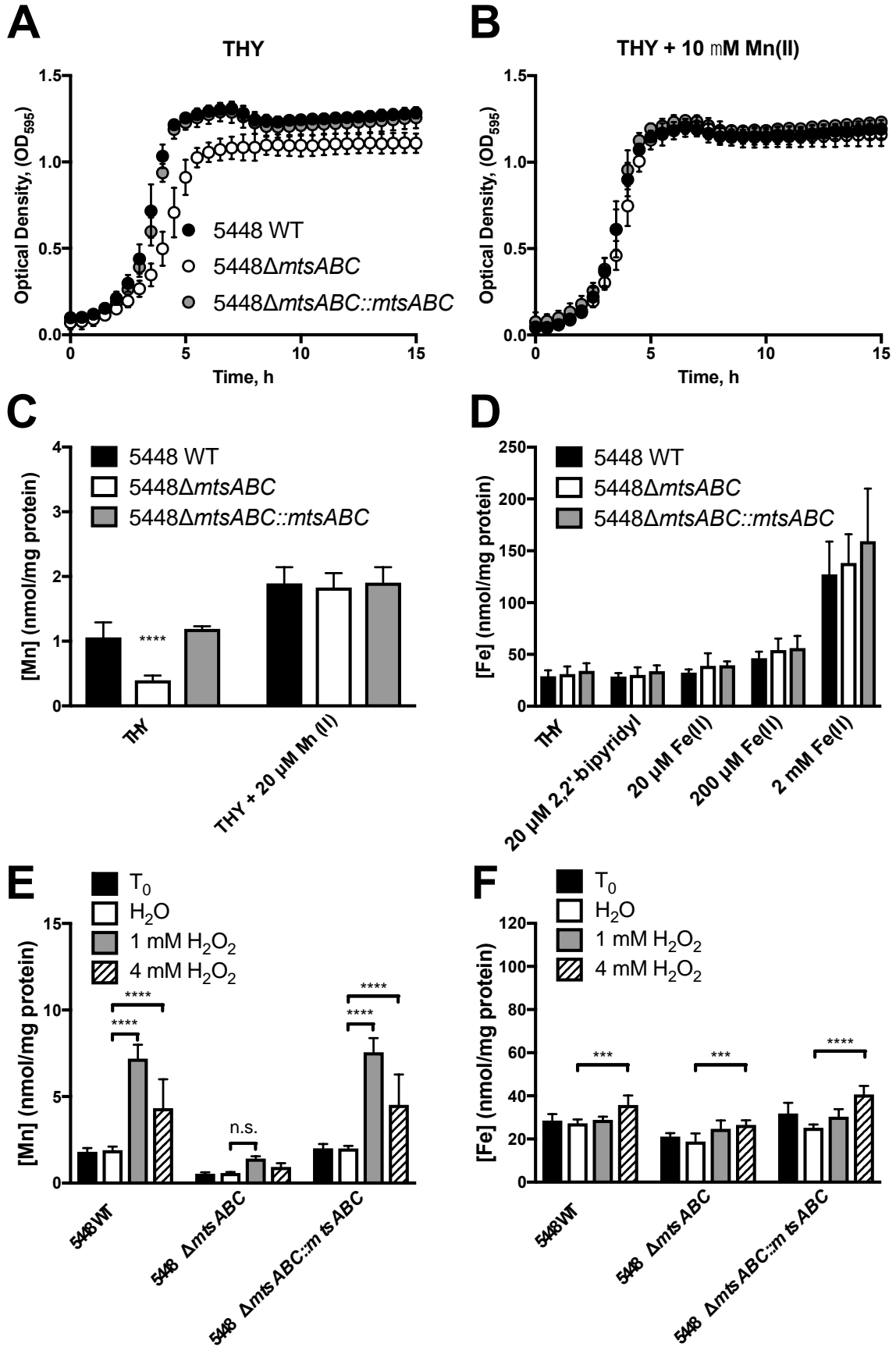
Figure 2 - Effect of mutation of *mtsABC* on intracellular metal accumulation and growth

Overnight cultures of 5448 WT (black circles), 5448Δ*mtsABC* (open circles) and 5448Δ*mtsABC::mtsABC* (grey circles) were diluted to OD_{600} = 0.05 into THY broth alone (**A**) or THY broth with 10 μM Mn(II) (**B**). Growth was monitored at 37 °C by recording the optical density at 595 nm (OD_{595}). WT (black bars), 5448Δ*mtsABC* (white bars) or 5448Δ*mtsABC::mtsABC* (grey bars) were grown in THY with or without 20 μM Mn(II) for intracellular Mn analysis (**C**) or in THY with or without 20 μM 2,2'-bipyridyl, 20 μM, 200 μM, or 2 mM Fe(II) for intracellular Fe analysis (**D**). Strains 5448 WT, 5448Δ*mtsA* and 5448Δ*mtsABC::mtsABC* were grown in THY at 37 °C to mid-exponential phase (OD_{600} 0.6 – 0.8) and challenged with H_2O, or with 1 mM or 4 mM H_2O_2, and total intracellular accumulation of Mn (**E**) or Fe (**F**) was measured by ICP-MS. Total metal content was normalised to protein content of the sample. Graphs represent mean ± standard deviation of 4 independent biological replicates. ((2-way ANOVA comparing strains to WT of that treatment or change due to treatment within strain, compared to H_2O as control, *** $P <$ 0.001, **** $P <$ 0.0001).

1
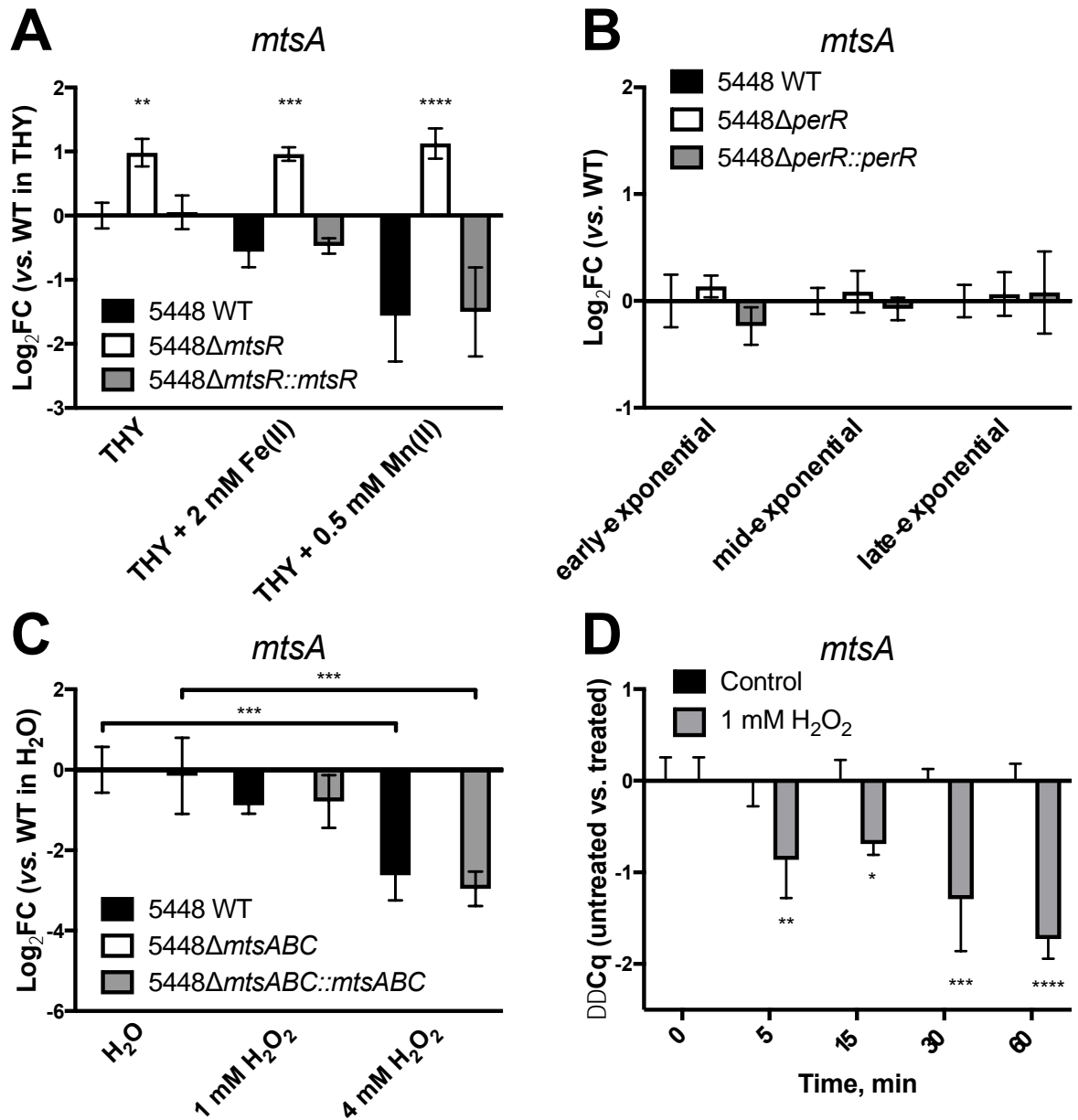
Figure 3 – Analysis of expression of *mtsA* in response to Fe, Mn and H₂O₂

5448 WT, 5448Δ*mtsR*, and 5448Δ*mtsR::mtsR* were grown at 37 °C to mid-exponential phase

($OD_{600} = 0.6$-0.8) in either THY alone or THY containing 2 mM Fe(II) or 0.5 mM Mn(II) and

expression of the *mtsA* gene was analysed (**A**). 5448 WT, 5448Δ*perR*, and 5448Δ*perR::perR*

were grown in THY at 37 °C to early-exponential ($OD_{600} = 0.3$), mid-exponential ($OD_{600} = $

0.6), or late-exponential ($OD_{600} = 0.9$) and expression of the *mtsA* gene was analysed (**B**).

5448 WT, 5448Δ*mtsABC*, 5448Δ*mtsABC::mtsABC* were grown in THY to mid-exponential

1   phase (OD_{600} = 0.6-0.8) in THY and challenged with H_2O, or with 1 mM or 4 mM H_2O_2, and

2   expression of the *mtsA* gene was analysed (**C**). 5448 WT was grown to mid-exponential

3   phase (OD_{600} = 0.6-0.8) in THY and challenged with either H_2O (black bars) or 1 mM H_2O_2

4   (grey bars) and expression of the *mtsA* gene was analysed at t = 0, 5, 15, 30 or 60 min (**D**).

5   *mtsA* expression was analysed by qPCR using *gyrA* as the reference gene. Data represent the

6   mean $\pm$ standard deviation of 3 independent biological replicates ((2-way ANOVA

7   comparing strains to WT of that treatment or change due to treatment within strain, compared

8   to H_2O as control, ** $P < 0.01$, *** $P < 0.001$, **** $P < 0.0001$).

9

1
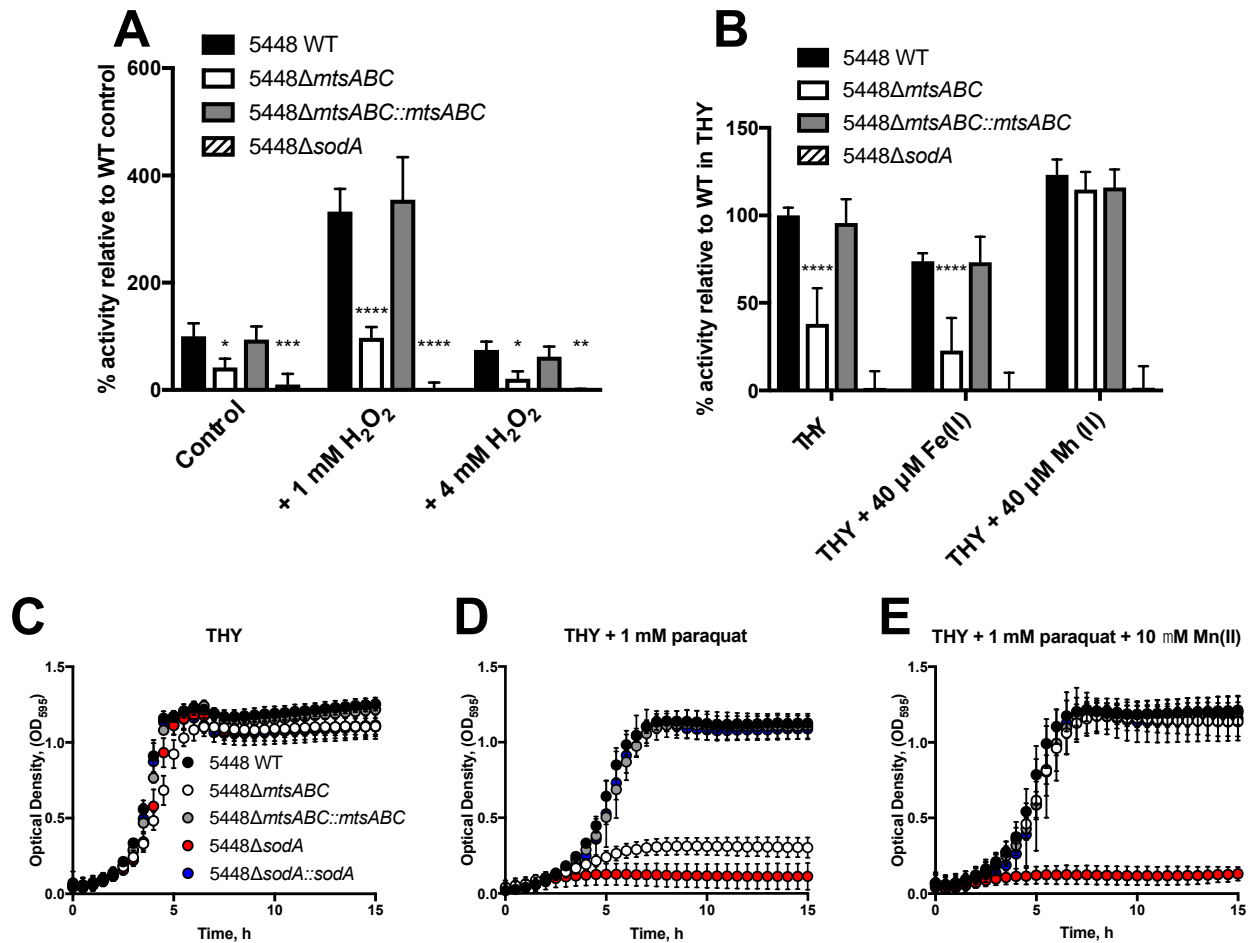
Figure 4 – Superoxide dismutase activity and sensitivity analysis of 5448Δ*mtsABC*

Strains 5448 WT, 5448Δ*mtsABC,* 5448Δ*mtsABC∷mtsABC* and 5448Δ*sodA* were grown in

THY at 37 °C to mid-exponential phase (OD$_{600}$ 0.6 – 0.8), challenged with either H$_2$O, 1 mM

H$_2$O$_2$, or 4 mM H$_2$O$_2$. Cells were harvested and SOD activity in cell extracts was analysed

(**A**). Strains 5448 WT, 5448Δ*mtsABC*, 5448Δ*mtsABC∷mtsAB,* and 5448Δ*sodA* were grown in

THY, THY + 40 μM Fe(II), or THY + 40 μM Mn(II) to mid-exponential growth phase

(OD$_{600}$ 0.6 – 0.8). Cells were harvested and SOD activity in cell extracts was analysed (**B**).

SOD activity in strains was normalised to 5448 WT in THY (or control) = 100% and activity

in the 5448Δ*sodA* mutant = 0%. (Raw data are shown in Figure S7). Overnight cultures of

5448 WT (black circles), 5448Δ*mtsABC* (open circles), 5448Δ*mtsABC::mtsABC* (grey

circles), 5448Δ*sodA* (red circles), and 5448Δ*sodA∷sodA* (blue circles) were diluted to OD$_{600}$

1   = 0.05 into THY broth alone (**C**), THY broth with 1 mM paraquat (**D**), or THY broth with 1

2   mM paraquat and 10 μM Mn(II) (**E**). Growth was monitored at 37 °C by recording the optical

3   density at 595 nm (OD$_{595}$). Graphs represent mean ± standard deviation of at least 3

4   independent biological replicates. ((2-way ANOVA comparing strains to WT of that

5   treatment or change due to treatment within strain, compared to H$_2$O as control , * $P < 0.05$,

6   ** $P < 0.01$,*** $P < 0.001$, **** $P < 0.0001$).

7

A

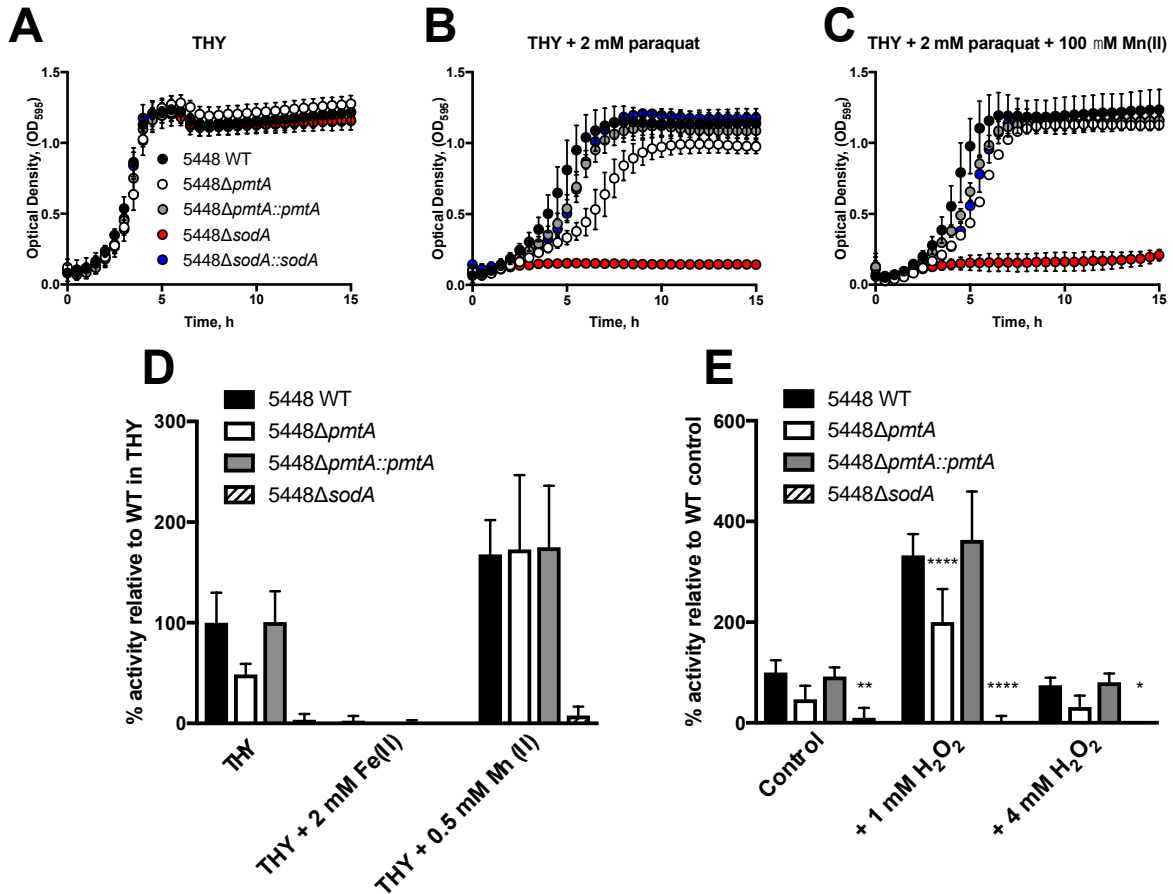|	Mn	Fe
rSodA-Fe	0.22±0.005	0.74±0.132
rSodA-Mn	1.24±0.229	0.06±0.079

B

1
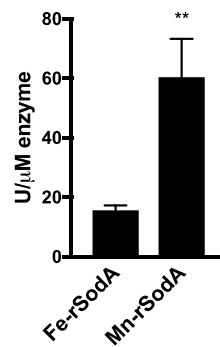
Figure 5 – Activity of recombinant SodA in Fe or Mn isoforms

Metal content of Fe-rSodA and Mn-rSodA isoforms (**A**). SOD activity in Fe-rSodA and Mn-rSodA isoforms (**B**). Data represent mean ± standard deviation of 3 biological replicates. (Student's *t*-test, ** $P < 0.01$).

2

Figure 6 – Superoxide sensitivity analysis and superoxide dismutase activity of

5448Δ*pmtA*

Strains 5448 WT, 5448Δ*pmtA*, 5448Δ*pmtA∷pmtA* and 5448Δ*sodA* were grown in THY, THY

+ 2 mM Fe(II), or THY + 0.5 mM Mn(II) to mid-exponential growth phase (OD_{600} 0.6 – 0.8.

Cells were harvested and SOD activity in cell-free extracts was analysed (**A**). 5448 WT,

5448Δ*pmtA*, 5448Δ*pmtA∷pmtA*, and 5448Δ*sodA* were grown in THY at 37 °C to mid-

exponential phase (OD_{600} 0.6 – 0.8), challenged with either H_2O, 1 mM H_2O_2 or 4 mM H_2O_2.

Cells were harvested and SOD activity was analysed (**B**). Activity in strains was normalised

to 5448 WT in THY (or control) = 100% and activity in the 5448Δ*sodA* mutant = 0% (Raw

data is in Figure S7). Overnight cultures of 5448 WT (black circles), 5448Δ*pmtA* (open

circles), 5448Δ*pmtA::pmtA* (grey circles), 5448Δ*sodA* (red circles), and 5448Δ*sodA∷sodA*

1 (blue circles) were diluted to $OD_{600} = 0.05$ into THY broth alone (**C**), THY broth with 2 mM

2 paraquat (**D**), or THY broth with 2 mM paraquat and 100 μM Mn(II) (**E**). Growth was

3 monitored at 37 °C by recording the optical density at 595 nm (OD_{595}). Graphs represent

4 mean ± standard deviation of at least 3 independent biological replicates. (2-way ANOVA

5 comparing strains to WT of that treatment or change due to treatment within strain, compared

6 to H_2O as control, $* P < 0.05$, $** P < 0.01$, $**** P < 0.0001$).

7
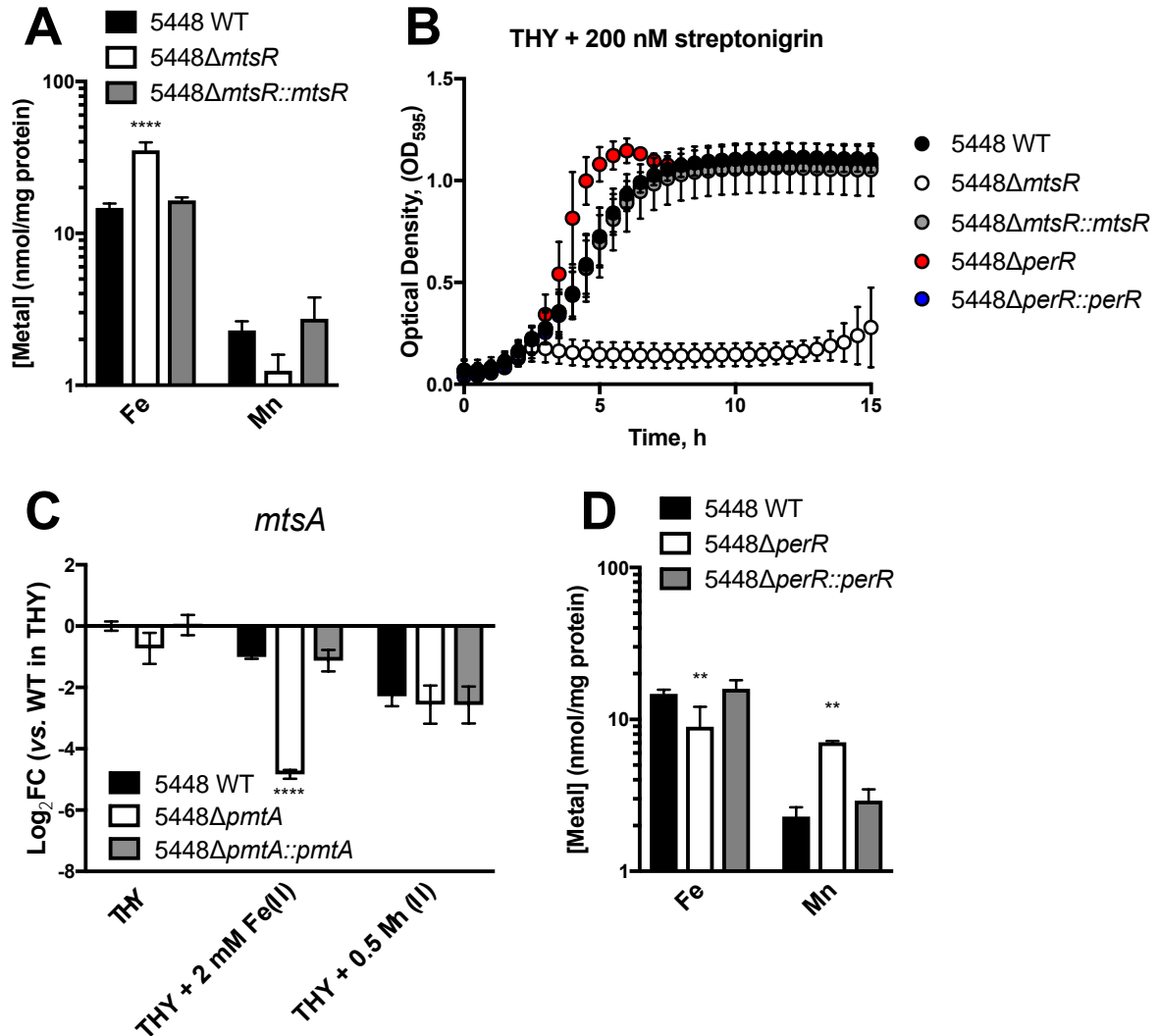
**Figure 7 – Fe and Mn content of *perR* and *mtsR* mutants and *mtsA* regulation in 5448Δ*pmtA***

Strains 5448 WT, 5448Δ*mtsR* and 5448Δ*mtsR::mtsR* were grown in THY at 37 °C to mid-exponential phase (OD_{600} 0.6 – 0.8) and analysed by ICP-MS for Fe and Mn (**A**). Total metal content was normalised to protein content of the sample. 5448 WT (black circles), 5448Δ*mtsR* (white circles), 5448Δ*mtsR::mtsR* (grey circles), 5448Δ*perR* (red circles), or 5448Δ*perR::perR* (blue circles) was diluted to $OD_{600} = 0.05$ into THY broth alone (Figure S10) or THY broth containing 200 nM streptonigrin (**B**). Growth was monitored at 37 °C by recording the optical density at 595 nm (OD_{595}). Strains 5448 WT, 5448Δ*pmtA*, and 5448Δ*pmtA::pmtA* were grown at 37 °C to mid-exponential phase ($OD_{600} = 0.6$-0.8) in either

1   THY alone, THY + 2 mM Fe(II), or 0.5 mM Mn(II), and expression of the *mtsA* gene was

2   analysed (**C**). *mtsA* expression was analysed by qPCR using *gyrA* as the reference gene.

3   Strains 5448 WT, 5448Δ*perR*, and 5448Δ*perR*∷*perR* were grown in THY at 37 °C to mid-

4   exponential phase (OD_{600} 0.6 – 0.8) and analysed by ICP-MS for Fe and Mn (**D**). Total metal

5   content was normalised to protein content of the sample. Graphs represent mean ± standard

6   deviation of 3 independent biological replicates. (1-way ANOVA used comparing all to 5448

7   WT or 2-way ANOVA comparing strains to WT, ** $P < 0.01$, **** $P < 0.0001$).

8
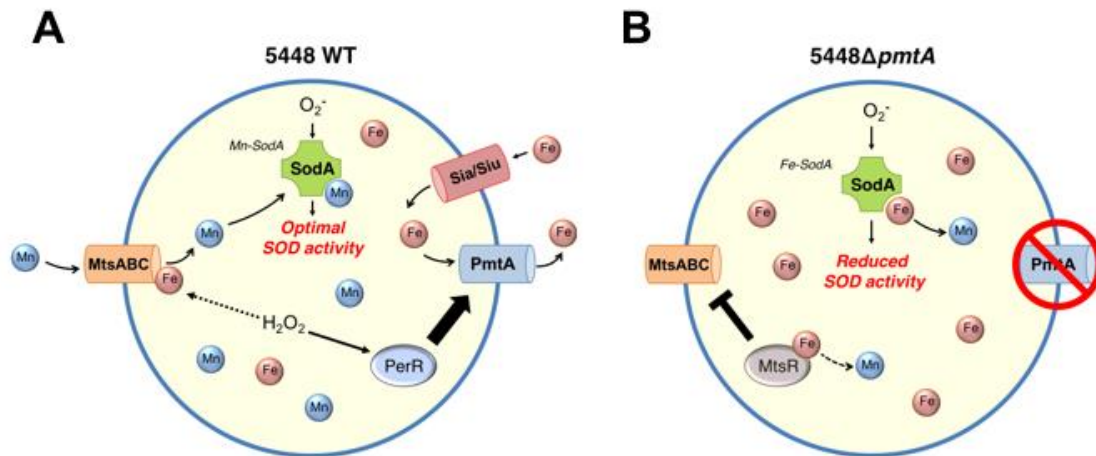
Figure 8 – Model of the interplay between Mn and Fe homeostasis and Sod metalation in 5448 WT and 5448Δ*pmtA*

During hydrogen peroxide stress conditions, H_2O_2 is sensed by PerR, leading to the upregulation of PmtA and subsequent efflux of Fe(II). At the same time, we hypothesise that Fe that is adventitiously bound to the cytoplasmic domains of MtsABC may become oxidized and dissociate, leading to increased Mn import (**A**). In the 5448Δ*pmtA* mutant, high intracellular Fe may result in dysregulation of MtsR and hence downregulation of Mn uptake by MtsABC. This combined high Fe, low Mn status may result in the generation of Fe-SodA, which has reduced activity compared to the Mn-cofactored form (**B**). Dashed lines denote hypothetical or putative mechanisms, while solid lines indicate mechanisms that have been confirmed experimentally. Thick arrows show upregulation, while a thick blocked arrow indicates repression.